

·专题研究·

藏南泽当岛弧花岗岩成因限定 ——来自角闪石岩锆石 U-Pb、地球化学和 Sr-Nd 同位素的证据

陈 翰^{1,2}, 胡古月², 郭英帅³, 王 莉⁴

(1. 成都理工大学 地球科学学院, 四川 成都 610059; 2. 中国地质科学院 矿产资源研究所, 自然资源部成矿作用与资源评价重点实验室, 北京 100037; 3. 山西能源学院 地质与测绘工程系, 山西 太原 030006; 4. 河南省有色金属地质勘查总院, 河南 郑州 450052)

摘要: 泽当岛弧位于藏南乃东县境内, 主要由英云闪长岩、花岗闪长岩、奥长花岗岩和角闪石岩组成, 是晚侏罗世洋壳俯冲的产物。本文对该地区出露的角闪石岩开展了野外地质调查, 通过室内 SHRIMP 锆石 U-Pb 定年、全岩地球化学和 Sr-Nd 同位素等研究, 探讨了泽当角闪石岩的成因、源区及其与花岗岩的成因关系, 获得以下认识: 角闪石岩成岩年龄为 159.1 ± 7.2 Ma; 角闪石岩具有较低 Sr 含量、较高的 Y 含量和较低的 Sr/Y 值, 富集 MREE; 角闪石岩与花岗岩 Sr-Nd 同位素特征一致, 角闪石岩 $^{87}\text{Sr}/^{86}\text{Sr}(t)$ 值 ($0.7040 \sim 0.7045$) 较低, $\varepsilon\text{Nd}(t)$ 值变化范围为 $+5.5 \sim +6.1$ 。结合前人研究认为, 泽当岛弧的英云闪长岩、花岗闪长岩、奥长花岗岩和角闪石岩均来自地幔楔部分熔融作用。英云闪长岩为相对原始的岩浆, 在角闪石分离结晶作用未结束前, 先从岩浆房中分离出来; 残余岩浆继续发生角闪石分离结晶作用, 导致 Sr/Y 值进一步升高和 Cr、Ni、MREE 含量进一步降低。因此, 角闪石的分离结晶作用是泽当岛弧高 Sr/Y 花岗岩形成的关键因素。

关键词: 泽当岛弧; 角闪石岩; 花岗岩; 分离结晶作用; 地球化学

中图分类号: P588.12; P597

文献标识码: A

文章编号: 1000-6524(2020)05-0511-14

Petrogenesis of the Zetang arc granite in southern Tibet: Evidence from zircon U-Pb dating, geochemistry and Sr-Nd isotopes of amphibolite

CHEN Han^{1,2}, HU Gu-yue², GUO Ying-shuai³ and WANG Li⁴

(1. College of Earth Science, Chengdu University of Technology, Chengdu 610059, China; 2. MRL Key Laboratory of Metallogeny and Mineral Assessment, Institute of Mineral Resources, Chinese Academy of Geological Sciences, Beijing 100037, China; 3. Department of Geological Engineering, Shanxi Institute of Energy, Taiyuan 030006, China; 4. Henan Academy of Nonferrous Metals Geological Exploration, Zhengzhou 450052, China)

Abstract: The Zetang island arc, located in Nedong County, southern Tibet, mainly consists of tonalite, trondhjemite, granodiorite and amphibolite. The Zetang island arc has been identified as a late Jurassic intra-oceanic arc. In this paper, integrated field geological survey, SHRIMP zircon U-Pb dating, whole rock geochemistry and Sr-Nd isotope study were carried out on the Zedang island arc to discuss magma source of amphibolite and its relationship with coeval granites. Some conclusions have been reached: ① SHRIMP zircon $^{206}\text{Pb}/^{238}\text{U}$ dating of amphibolite shows a crystallization age of 159.1 ± 7.2 Ma; ② Sr-Nd isotopic characteristics of amphibolite and granites are similar, with $^{87}\text{Sr}/^{86}\text{Sr}(t)$ ratios being $0.7040 \sim 0.7045$ and $\varepsilon\text{Nd}(t)$ values being $+5.5 \sim +6.1$. ③ geochemical

收稿日期: 2019-10-24; 接受日期: 2020-06-03; 编辑: 郝艳丽

基金项目: 国家重点研发计划-深地专项(2018YFC0604106); 国家自然科学基金项目(41503006); 中国地质调查局二级项目(DD20190167)

作者简介: 陈 翰(1991-), 男, 博士研究生, 矿物学、岩石学、矿床学专业, E-mail: ChenHan330238@163.com; 通讯作者: 胡古月(1985-), 男, 副研究员, 主要从事同位素地球化学及构造地球化学研究, E-mail: wanghuguyue@126.com。

characteristics show low Sr, high Y, low Sr/Y ratio, and enrichment of MREE. A comparison with other published data shows that tonalite, trondhjemite, granodiorite and amphibolite of Zetang arc were likely derived from the partial melting of the mantle wedge. Tonalite is a relatively primitive magma, and had been separated from the magma chamber before the full completion of amphibolite fractional crystallization. With the ongoing crystallization of amphibolite, the Sr/Y ratios, Cr, Ni and MREE values of residual magma increased step by step. Therefore, the fractional crystallization of amphibolite seems to have been the key factor for forming the high Sr/Y granites of Zetang island arc.

Key words: Zetang island arc; amphibolite; granite; fractional crystallization; geochemistry

Fund support: National Key Research and Development Program of China (2018YFC0604106); National Natural Science Foundation of China (41503006); China Geological Survey Project (DD20190167)

大型洋盆(如太平洋和特提斯洋)的消减过程会形成洋内岛弧,典型的有西南太平洋岛弧(Oliver and Isacks, 1967; Isacks *et al.*, 1968; Stern *et al.*, 2003; Smith and Price, 2006; Takahashi *et al.*, 2007, 2008),北美的Alaska岛弧、Talkeetna岛弧等(Bard, 1983; DeBari and Coleman, 1989; Burg *et al.*, 1998; Greene *et al.*, 2006; Garrido *et al.*, 2006; Dhuime *et al.*, 2007; Kelemen *et al.*, 2007; DeBari and Greene, 2011; Burg, 2011)。大洋消亡-碰撞造山过程中,洋内岛弧可能随板块运动拼贴到大陆边缘,最终就位于缝合带中,也可能随俯冲带一起消失。特提斯构造域中目前已发现了Kohistan(Arbaret *et al.*, 2000; Garrido *et al.*, 2006)、雄村(Lang *et al.*, 2014; Tang *et al.*, 2015)和泽当等洋内弧(Aitchison *et al.*, 2000, 2007; McDermid *et al.*, 2002)。

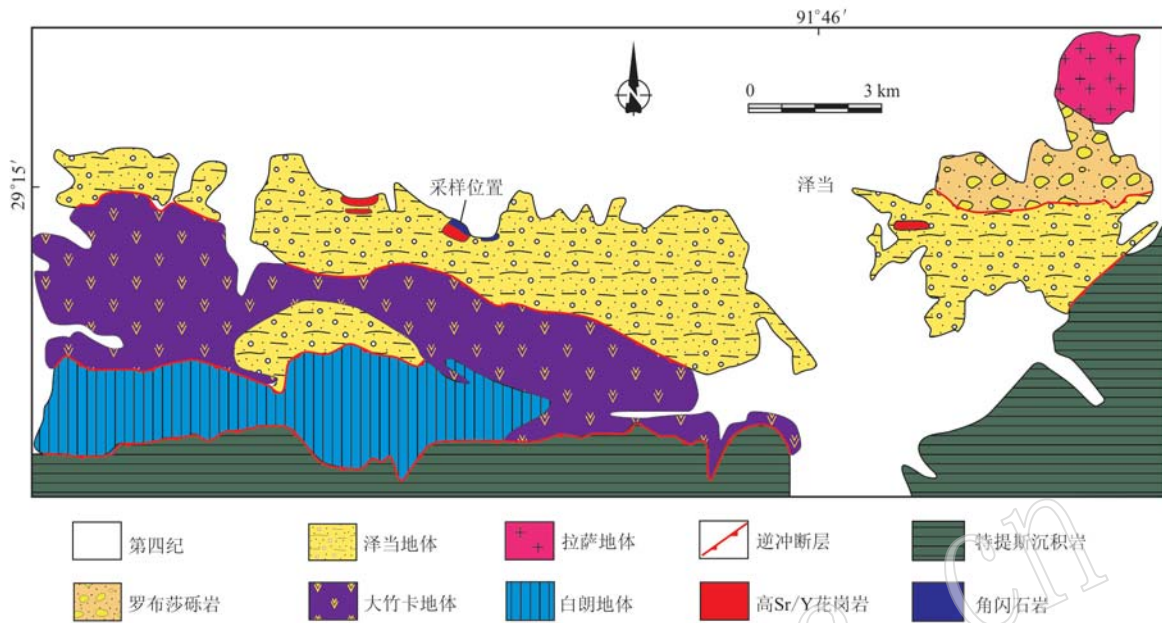
泽当岛弧及其南侧的蛇绿岩套形成于洋壳俯冲背景,是青藏高原雅鲁藏布江缝合带中出露面积较大、保存较好的岛弧(Aitchison *et al.*, 2000, 2007; McDermid *et al.*, 2002; 韦栋梁等, 2004, 2006, 2007; 王莉等, 2012; 刘维亮等, 2013; 李强等, 2014; 赵珍等, 2014)。泽当岛弧主要由具有高Sr/Y值特征的花岗岩(英云闪长岩、花岗闪长岩、奥长花岗岩)组成,形成年龄在 $161 \pm 2.3 \sim 152.5 \pm 1.3$ Ma之间,地球化学特征显示其形成于俯冲背景,形成过程中可能经历了角闪石分离结晶作用(McDermid *et al.*, 2002; 韦栋梁等, 2007; 王莉等, 2012; 赵珍等, 2014)。另有观点认为,花岗质的泽当地体属于新特提斯洋向欧亚大陆北向俯冲形成的陆缘弧岩浆岩的一部分,为含水玄武质岩浆底侵增厚新生下地壳的产物(Zhang *et al.*, 2014)。

中地壳层以下的角闪石分离结晶作用会影响弧岩浆岩的地球化学特征,但由于弧岩浆岩演化中形

成的堆晶岩很少出露于地表,使得角闪石分离结晶作用显得十分神秘(Davidson *et al.*, 2007; Jeff and Dante, 2010; Smith, 2014)。前人对泽当岛弧出露的角闪石岩研究较为薄弱,元素地球化学特征表明角闪石岩与花岗岩可能为同一岩浆系统内不同阶段结晶的产物(王莉等, 2012),但缺乏基础的岩石学、矿物学研究以及高精度的锆石U-Pb定年和Sr-Nd同位素证据。本文对泽当岛弧角闪石岩开展了野外地质调查和镜下光薄片观察,进行了SHRIMP锆石U-Pb定年、全岩地球化学和Sr-Nd同位素分析等工作,获得了高质量的年代学、地球化学及同位素地球化学数据,为限定泽当岛弧中角闪石岩和花岗岩的成因提供了新的地球化学证据。

1 地质背景

雅鲁藏布江缝合带东段乃东县泽当镇附近,自北向南分布着泽当地体、大竹卡地体和白朗地体(图1),分别代表了残留洋弧、弧前蛇绿岩和俯冲增生杂岩(Aitchison *et al.*, 2000; 王莉等, 2012),三者由一套逆冲推覆系统控制(Yin *et al.*, 1994, 1999; Quidelleur *et al.*, 1997; Harrison *et al.*, 2000)。最北侧的泽当地体由Aitchison(Aitchison *et al.*, 2000)首次命名,亦被称为泽当地质窗(Harrison *et al.*, 2000)或泽当岛弧(McDermid *et al.*, 2002)。泽当残留洋弧为一套长12 km、面积 25 km^2 左右的晚侏罗世洋内俯冲岩石组合,主要出露的侵入岩有英云闪长岩、花岗闪长岩、奥长花岗岩和角闪石岩。以英云闪长岩、花岗闪长岩、奥长花岗岩为代表的高Sr/Y花岗岩,形成年代在 $161 \sim 152$ Ma之间,被认为是晚侏罗世新特提斯洋向北俯冲的产物(McDermid *et al.*, 2002; 韦栋梁等, 2007; 王莉等, 2012; 赵珍

图 1 泽当地区地质简图(据 McDermid *et al.*, 2002)Fig. 1 Simplified map showing the location and geology of Zetang area (after McDermid *et al.*, 2002)

等, 2014)。泽当角闪石岩出露于泽当镇西侧约 2~3 km 处, 不连续的角闪石岩露头在南北向上约 100 m 宽, 与高 Sr/Y 花岗岩伴生, 东西向展布于泽当地体北侧(图 2a)。角闪石岩与花岗闪长岩出露位置最近, 产于花岗闪长岩的下部, 奥长花岗岩出露于角闪石岩西侧约 1~1.5 km 处, 英云闪长岩与角闪石岩出露位置最远, 出露于角闪石岩东侧约 5 km 处。

2 样品采集及描述

角闪石岩呈黑绿色, 中粗粒粒状结构, 块状构造(图 2b), 主要矿物为角闪石, 含量占 90% 以上, 次要矿物为斜长石, 含量约 8% 左右。角闪石呈长柱状, 长宽比大于 3:1, 粒径不等, 在 1~5 mm 左右, 蚀变较弱, 表面发育少量绿泥石化。镜下观察角闪石多色性为棕色-浅绿色(图 2d), 自形-半自形结构, 自形程度较高。正高突起, 可见明显两组完全解理, 解理角 56°(图 2c)。

野外采样过程中为避免角闪石岩样品中混入花岗闪长岩脉, 选择在远离(约 20 m)花岗闪长岩脉处采集了角闪石岩全岩地球化学样品 7 件(TD133-1~TD133-7)、Sr-Nd 同位素样品 6 件(TD133-2~TD133-7)、SHRIMP 锆石 U-Pb 同位素样品 1 件(TD133)。

3 测试分析

3.1 主量和微量元素分析

泽当角闪石岩主量及微量元素测试在国土资源部国家地质实验测试中心进行。主量元素采用 XRF 方法和湿化学法测定, 测试仪器为 X 荧光光谱仪 3080E, 测试精度 5%。微量元素和稀土元素采用等离子质谱仪(ICP-MS-Excell) 分析, 含量大于 10×10^{-6} 的元素的测试精度为 5%, 含量小于 10×10^{-6} 的元素精度为 10%, 个别含量较低的元素, 测试误差超过 10%, 详细的原理及测试过程可参考卓尚军等(2003) 和吉昂(2012)。

3.2 SHRIMP 锆石 U-Pb 同位素定年

测年角闪石岩样品 TD-133 的锆石挑选工作在河北省区域地质矿产调查研究所进行。挑出的锆石在中国地质科学院地质研究所经制靶、抛光后, 于北京离子探针中心进行阴极发光显微照相, 排除裂纹较多、环带不清晰的锆石, 选取晶型完整、具有代表性的锆石进行测试分析。锆石 U-Pb 同位素定年测试在北京离子探针中心采用离子探针 SHRIMP II 型测试仪进行。标样为 TEM 锆石, 测试过程中每测定 3 个未知点, 插入一次标样测定, 以及时校正误差, 保障测试精度, 详细的实验过程可参考宋彪(2015)。角闪石岩锆

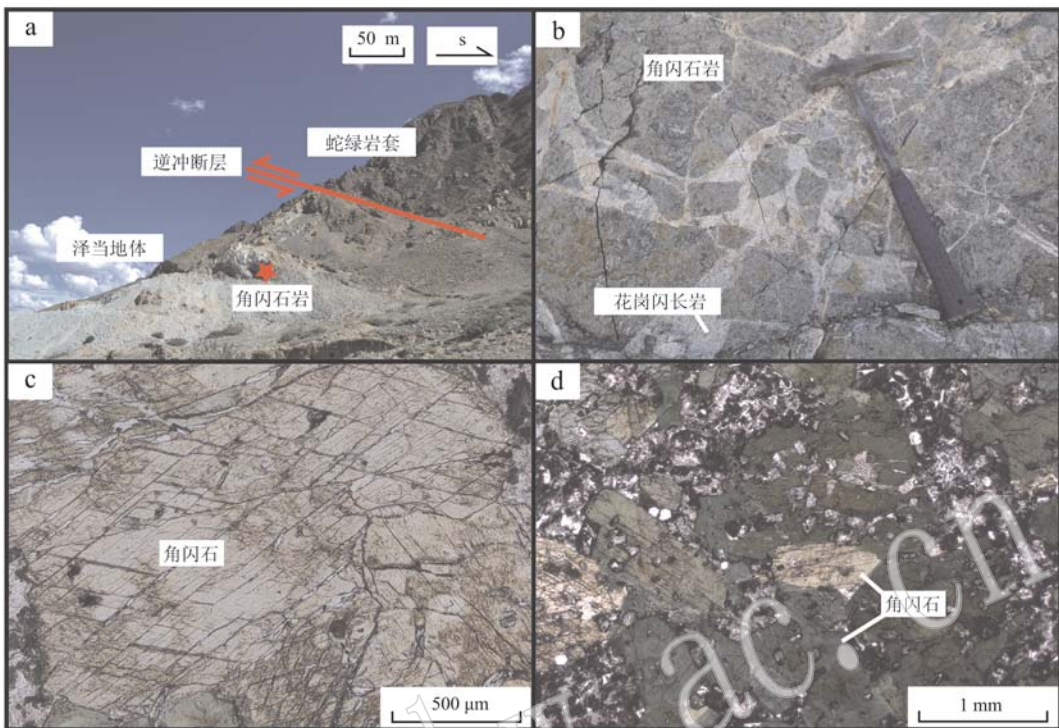


图2 泽当角闪石岩的野外(a,b)和单偏光下显微照片(c,d)

Fig. 2 Field Photographs (a, b) and microphotographs under plainlight (c, d) of Zetang magmatic amphibolite

石 U-Pb 同位素测年实验的数据处理、年龄计算采用 ISOPLOT 3.0 程序 (Ludwig, 2003)。

3.3 Sr-Nd 同位素分析

角闪石岩全岩 Sr-Nd 同位素测试在中国科学技术大学壳幔物质与环境重点实验室进行, 所用气体质谱仪器为 Finnigan MAT-262。标准溶液 NBS987 的重复测量结果为 $^{87}\text{Sr}/^{86}\text{Sr} = 0.710\,249 \pm 0.000\,012$ (2σ , $n = 38$) , 标准溶液 La Jolla 的重复测量结果为 $^{143}\text{Nd}/^{144}\text{Nd} = 0.511\,869 \pm 0.000\,006$ (2σ , $n = 25$) 。Sr 和 Nd 同位素比值测量精度优于 0.003%。测量得到的同位素比值采用 $^{86}\text{Sr}/^{88}\text{Sr} = 0.119\,4$ 和 $^{146}\text{Nd}/^{144}\text{Nd} = 0.721\,9$ 进行质量分馏校正。重复分析标准溶液 NBS 987 和 La Jolla, 分别得到 $^{87}\text{Sr}/^{86}\text{Sr}$ 值为 $0.710\,249 \pm 0.000\,012$ 和 $^{143}\text{Nd}/^{144}\text{Nd}$ 值 $0.511\,869 \pm 0.000\,006$ 。 $\varepsilon_{\text{Nd}}(t)$ 值计算参考 SHRIMP 镶石 U-Pb 同位素定年结果 159 Ma 进行计算。详细的实验过程可参考 Chen 等(2000, 2002, 2007)。

4 测试分析结果

4.1 主量和微量元素地球化学特征

角闪石岩的主量和微量元素分析结果列于表 1。

泽当角闪石岩样品 SiO_2 和 Al_2O_3 含量较低, 分别为 44.49% ~ 47.92% 和 11.63% ~ 17.61%; TiO_2 、 FeO^+ 、 MnO 、 MgO 四者含量较高, TiO_2 含量为 0.73% ~ 0.95%, FeO^+ 含量为 8.48% ~ 10.00%, MnO 含量为 0.17% ~ 0.21%, MgO 含量为 6.55% ~ 14.87%; 样品 $\text{K}_2\text{O}/\text{Na}_2\text{O}$ 值较低, 为 0.13 ~ 0.85; $\text{Mg}^{\#}$ 值较高(57.0 ~ 73.0), 平均值 69.0。

泽当角闪石岩 Sr (355×10^{-6} ~ $1\,150 \times 10^{-6}$) 含量较低, Y 含量 (13.2×10^{-6} ~ 22.9×10^{-6}) 较高, Sr/Y 值 [23.8 ~ 74.7, 剔除特高值 74.7(TD133-2), 平均值 31.8] 较低; Cr 、 Ni 含量较高, 分别为 119×10^{-6} ~ 724×10^{-6} (平均值 576×10^{-6}) 和 54×10^{-6} ~ 344×10^{-6} (平均值 242×10^{-6}); Nb 含量为 1.06×10^{-6} ~ 3.19×10^{-6} , Nb/Y 值为 0.59 ~ 1.12, Zr 含量为 24.4×10^{-6} ~ 56.2×10^{-6} , Zr/TiO_2 值为 0.003 18 ~ 0.006 69。

泽当角闪石岩 ΣREE 含量 37.2×10^{-6} ~ 82.0×10^{-6} , 稀土元素含量较低。 LREE/HREE 和 $(\text{La}/\text{Yb})_N$ 值分别在 3.12 ~ 6.79 和 2.31 ~ 7.87 之间, 轻重稀土元素分异程度不高, 稀土元素球粒陨石标准化分布图为右倾平缓型(图 3a); 原始地幔标准化蛛网图显示亏损 P、Nb、Ce、Ta、Ti 等高场强元素, 富集 Rb、K、Ba、U

表 1 角闪石岩主量($w_B/\%$)、微量元素($w_B/10^{-6}$)分析结果Table 1 Major elements ($w_B/\%$), trace elements and rare earth elements ($w_B/10^{-6}$) geochemical characteristics of magmatic amphibolite

样品号	TD133-1	TD133-2	TD133-3	TD133-4	TD133-5	TD133-6	TD133-7	样品号	TD133-1	TD133-2	TD133-3	TD133-4	TD133-5	TD133-6	TD133-7
SiO ₂	47.55	47.92	44.49	44.51	44.95	44.74	44.54	Ba	673	493	531	415	384	619	753
TiO ₂	0.88	0.84	0.95	0.84	0.90	0.73	0.78	Dy	4.01	2.77	3.33	2.69	2.91	2.56	2.53
Al ₂ O ₃	17.61	14.71	13.05	12.93	11.63	13.66	12.68	Hf	2.07	2.10	1.48	1.14	1.29	1.10	1.09
FeO	5.80	4.62	6.20	5.95	6.27	5.69	5.91	Ta	0.17	0.14	0.10	0.07	0.07	0.08	0.08
Fe ₂ O ₃	3.66	4.29	4.03	4.12	4.15	4.25	4.30	W	0.11	0.21	0.13	0.07	0.07	0.05	0.07
MnO	0.20	0.20	0.21	0.17	0.18	0.17	0.18	Tl	0.20	<0.05	0.13	0.08	0.05	0.12	0.09
MgO	6.55	9.39	14.15	14.04	14.87	13.26	14.44	Pb	5.11	11.4	1.32	1.46	0.79	2.38	4.06
CaO	10.63	11.69	10.73	11.90	11.40	11.83	11.38	Th	2.37	4.41	0.63	0.76	0.78	0.70	0.89
Na ₂ O	2.48	2.16	1.17	1.28	1.33	1.17	1.18	U	1.63	1.36	0.22	0.23	0.31	0.21	0.28
K ₂ O	1.70	0.28	0.99	0.87	0.72	1.00	0.85	La	13.0	16.1	5.76	5.44	5.96	4.99	5.66
P ₂ O ₅	0.25	0.22	0.06	0.07	0.07	0.05	0.06	Ce	26.6	29.2	13.7	11.0	12.2	10.2	11.4
LOI	1.75	2.58	2.49	1.80	1.89	2.16	2.54	Pr	3.64	3.84	2.11	1.62	1.81	1.53	1.71
Total	99.06	98.90	98.52	98.48	98.36	98.71	98.84	Nd	18.3	17.4	11.9	8.40	9.37	8.34	8.61
Mg [#]	57.0	67.0	72.0	72.0	72.0	72.0	73.0	Sm	4.01	3.72	3.12	2.26	2.57	2.33	2.57
FeO ^t	9.09	8.48	9.83	9.66	10.00	9.51	9.78	Eu	1.38	1.14	1.05	0.84	0.90	0.85	0.91
Sc	33.7	35.1	35.6	48.0	47.4	37.6	48.1	Gd	4.21	3.39	3.42	2.75	2.88	2.52	2.53
V	338	288	324	318	341	291	301	Tb	0.72	0.53	0.61	0.49	0.52	0.45	0.46
Cr	119	400	700	724	721	652	716	Ho	0.86	0.55	0.66	0.52	0.57	0.51	0.52
Ni	54	167	283	282	299	265	344	Er	2.32	1.49	1.79	1.36	1.49	1.29	1.34
Co	32.3	35.2	51.8	53.8	55.4	50.8	56.0	Tm	0.35	0.22	0.27	0.20	0.22	0.21	0.20
Cu	5.9	19.6	7.1	27.4	22.9	16.6	26.4	Yb	2.25	1.38	1.68	1.29	1.37	1.22	1.21
Zn	78.3	82.7	78.7	63.5	63.2	67.0	69.5	Lu	0.32	0.19	0.24	0.18	0.19	0.17	0.17
Ga	18.4	19.7	13.9	13.4	12.8	13.8	13.5	Sr/Y	33.3	74.7	26.4	33.7	23.8	41.0	32.3
Rb	35.5	5.0	25.0	15.0	9.9	22.1	16.5	ΣREE	82.0	81.9	49.6	39.0	43.0	37.2	39.8
Sr	763	1 150	449	478	355	541	442	LREE	66.9	71.4	37.6	29.6	32.8	28.2	30.9
Y	22.9	15.4	17.0	14.2	14.9	13.2	13.7	HREE	15.0	10.5	12.0	9.5	10.2	8.9	9.0
Zr	50.5	56.2	30.3	25.7	28.7	24.4	26.1	LREE/HREE	4.45	6.79	3.14	3.12	3.23	3.16	3.44
Nb	3.19	2.71	1.76	1.10	1.29	1.06	1.13	(La/Yb) _N	3.90	7.87	2.31	2.84	2.93	2.76	3.15
Sn	0.90	1.08	0.79	0.64	0.83	0.60	0.66	δEu	1.02	0.96	0.98	1.03	1.01	1.07	1.08
Cs	1.00	0.23	0.51	0.34	0.23	0.64	0.40	δCe	0.92	0.87	0.95	0.88	0.89	0.88	0.87

注: $\delta\text{Eu} = \text{Eu}_N / (\text{Sm}_N / \text{Gd}_N)^{1/2}$, $\delta\text{Ce} = \text{Ce}_N / (\text{La}_N / \text{Pr}_N)^{1/2}$; $(\text{La} / \text{Yb})_N$ 为球粒陨石标准化后的比值(标准化数据引自 McDonough and Sun, 1995); $\text{Mg}^{\#} = 100 \times n(\text{Mg}^{2+}) / n(\text{Mg}^{2+} + \text{Fe}^{2+})$ 。

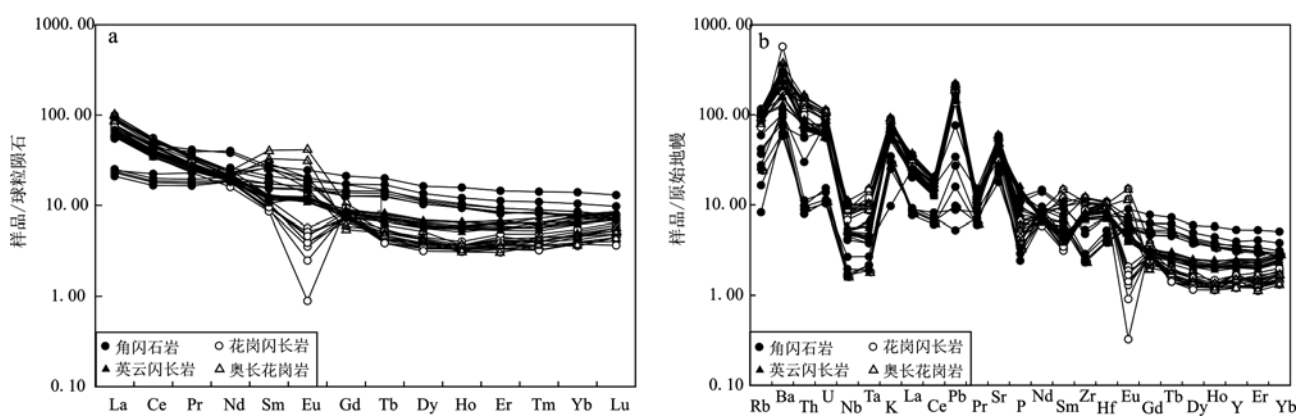


图 3 泽当角闪石岩和高 Sr/Y 花岗岩稀土元素球粒陨石标准化图(a)和微量元素原始地幔标准化蛛网图(b)(标准化数据引自 McDonough and Sun, 1995)

Fig. 3 Rare earth element distribution diagram (a) and trace element distribution diagram (b) of Zetang magmatic amphibolite and high Sr/Y granites magmatic rocks (after McDonough and Sun, 1995)

英云闪长岩数据引自韦栋梁等(2007); 花岗闪长岩数据引自王莉等(2012); 奥长花岗岩数据引自赵珍等(2014)

the data of tonalite from Wei Dongliang et al., 2007; the data of granodiorite from Wang Li et al., 2012; the data of trondhjemite from Zhao Zhen et al., 2014

等大离子亲石元素(图3b),具明显的岛弧型弧岩浆岩特征(赵珍等,2014)。

4.2 锆石U-Pb年代学

角闪石岩样品TD133-8中锆石呈长柱状,自形-半自形粒状结构,晶型较好,可见明显锆石环带(图4a)。测年锆石SHRIMP U-Pb同位素定年测试结果见表2。测年锆石Th和U含量分别在 42×10^{-6} ~ 834×10^{-6} 和 149×10^{-6} ~ 2100×10^{-6} 之间, Th/U值0.28~0.80,均大于0.2,矿物学及矿物地球化学特征显示测年锆石为典型岩浆锆石。

测试过程中总共选取10颗锆石进行了19个点

位测试,其中锆石测试点TD133-4.1的 $^{207}\text{Pb}/^{206}\text{Pb}$ 值明显高于其余测试点,说明普通铅(^{206}Pb)可能丢失,导致测年结果 1789 ± 15.0 Ma偏大,故将该数据剔除,以剩余的18个测点的年龄数据进行计算,结果显示锆石谐和年龄为 159.1 ± 7.2 Ma($n=18$)(图4b),MSWD=0.109,拟合程度高, $^{206}\text{Pb}/^{238}\text{U}$ 加权平均年龄为 159.8 ± 2.3 Ma($n=18$)(图4c)。泽当角闪石岩测年结果显示锆石谐和年龄和锆石加权平均年龄存在不一致,推测可能为后期少量流体作用引起的铅丢失,导致谐和年龄小于加权平均年龄,但二者误差<1%,属正常范围,以谐和年龄为准。

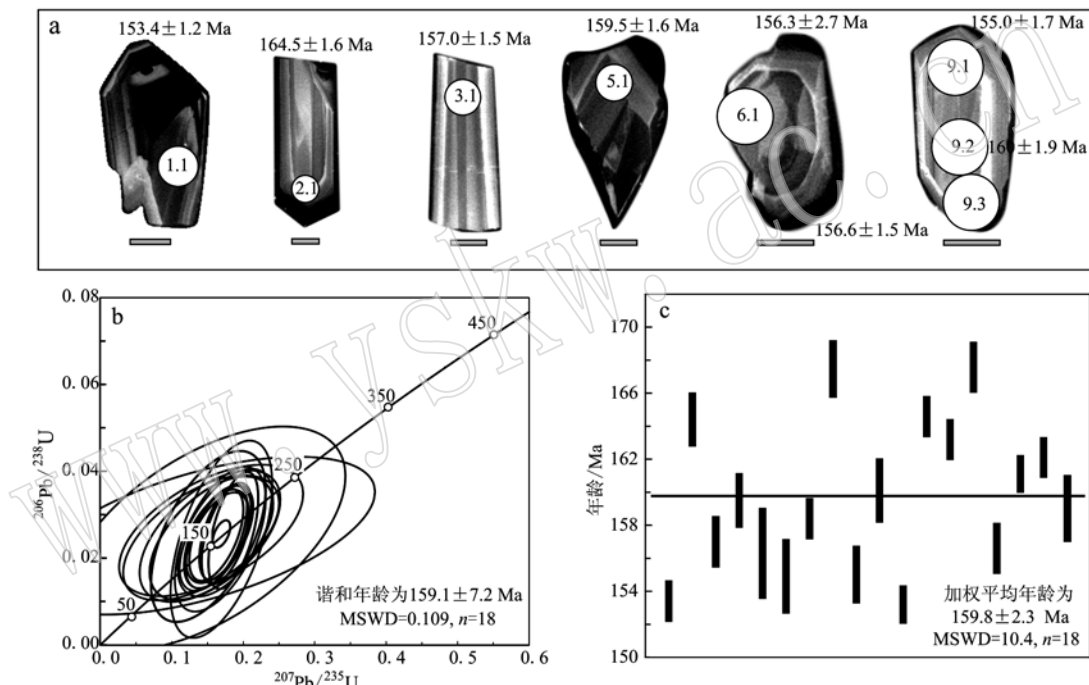


图4 泽当角闪石岩锆石CL图(a)、SHRIMP锆石U-Pb谐和图(b)和年龄分布图(c)

Fig. 4 CL photographs of zircon from Zedang magmatic amphibolite (a) and U-Pb concordia (b) and age distribution (c) diagrams of SHRIMP zircon U-Pb analytical results of Zetang magmatic amphibolite

4.3 Sr-Nd同位素

泽当角闪石岩总共分析了6件Sr-Nd同位素样品,测试结果见表3。分析结果显示,泽当角闪石岩具有较低的Rb含量(5.0×10^{-6} ~ 25.0×10^{-6}),较高的Sr含量(355×10^{-6} ~ 1150×10^{-6}),较高的Sm含量(2.26×10^{-6} ~ 3.72×10^{-6})和较高的Nd含量(8.3×10^{-6} ~ 17.4×10^{-6})。Rb/Sr=0.004~0.056, Sm/Nd=0.214~0.299, $^{143}\text{Nd}/^{144}\text{Nd}=0.512\ 882$ ~ $0.512\ 903$, $^{87}\text{Sr}/^{86}\text{Sr}=0.704\ 2$ ~ $0.704\ 7$, $\varepsilon\text{Nd}(t)=+5.5$ ~ $+6.1$ 。

泽当角闪石岩 $^{87}\text{Sr}/^{86}\text{Sr}$ 值、 $^{143}\text{Nd}/^{144}\text{Nd}$ 值与花岗闪长岩 $^{87}\text{Sr}/^{86}\text{Sr}$ 值(0.704 469~0704 864)、 $^{143}\text{Nd}/^{144}\text{Nd}$ 值(0.512 789~0.513 016)接近, $\varepsilon\text{Nd}(t)$ 值与花岗闪长岩 $\varepsilon\text{Nd}(t)$ 值(+5.1~+6.1)接近(王莉等,2012)。泽当角闪石岩 $^{87}\text{Sr}/^{86}\text{Sr}$ 值、 $^{143}\text{Nd}/^{144}\text{Nd}$ 值与英云闪长岩 $^{87}\text{Sr}/^{86}\text{Sr}$ 值(0.704 765~0.705 020)、 $^{143}\text{Nd}/^{144}\text{Nd}$ 值(0.512 789~0.513 016)接近, $\varepsilon\text{Nd}(t)$ 值小于英云闪长岩的 $\varepsilon\text{Nd}(t)$ 值(+6.7~+7.3)(韦栋梁等,2007)(表4)。

表 2 角闪石岩 SHRIMP 锆石 U-Pb 同位素测年数据

Table 2 SHRIMP zircon U-Pb isotopic data of magmatic amphibolite

测试点	$w_B/10^{-6}$			Th/U	$^{207}\text{Pb}/^{206}\text{Pb}$	1σ	$^{207}\text{Pb}/^{235}\text{U}$	1σ	$^{206}\text{Pb}/^{238}\text{U}$	1σ	$^{206}\text{Pb}/^{238}\text{U}$ 年龄/Ma $\pm 1\sigma$	不谐和 程度/%
	U	Th	^{206}Pb									
TD133-1.1	850	662	17.7	0.78	0.050 9	1.8	0.159 4	3.2	0.024 1	0.8	153.4 ± 1.2	-55
TD133-2.1	586	402	13.0	0.69	0.052 0	2.2	0.174 7	4.4	0.025 8	1.0	164.5 ± 1.6	-10
TD133-3.1	498	318	10.7	0.64	0.050 9	2.4	0.141 0	7.2	0.024 7	1.0	157.0 ± 1.5	160
TD133-4.1	149	42	41.2	0.28	0.115 7	0.8	4.943 0	1.5	0.319 9	1.0	1789.0 ± 15.0	2
TD133-5.1	377	229	8.21	0.61	0.053 0	2.7	0.153 4	6.5	0.025 1	1.0	159.5 ± 1.6	282
TD133-6.1	303	157	6.55	0.52	0.063 3	3.6	0.146 0	13.0	0.024 6	1.7	156.3 ± 2.7	199
TD133-7.1	460	225	9.64	0.49	0.053 2	2.4	0.169 4	4.7	0.024 3	1.5	154.9 ± 2.2	29
TD133-8.1	786	628	16.9	0.80	0.050 3	1.9	0.163 9	3.1	0.024 9	0.8	158.4 ± 1.2	-80
TD133-8.2	522	246	12.0	0.47	0.052 5	2.4	0.155 0	8.5	0.026 4	1.0	167.6 ± 1.7	190
TD133-9.1	370	175	7.79	0.47	0.055 2	3.0	0.167 8	4.2	0.024 3	1.1	155.0 ± 1.7	21
TD133-9.2	736	340	16.2	0.46	0.053 5	2.4	0.142 0	16.0	0.025 2	1.2	160.1 ± 1.9	155
TD133-10.1	2 100	834	43.5	0.40	0.052 1	2.0	0.163 2	2.9	0.024 1	0.7	153.2 ± 1.1	3
TD133-8.3	611	401	13.6	0.66	0.049 1	1.8	0.171 9	2.2	0.025 9	0.7	164.7 ± 1.2	-52
TD133-7.2	543	279	12.0	0.51	0.050 8	2.0	0.176 5	2.3	0.025 7	0.8	163.3 ± 1.2	14
TD133-7.3	426	204	9.63	0.48	0.050 1	2.1	0.186 1	2.3	0.026 4	0.9	167.7 ± 1.5	33
TD133-9.3	363	167	7.71	0.46	0.051 3	2.4	0.155 4	5.7	0.024 6	0.9	156.6 ± 1.5	1 606
TD133-11.1	1 211	614	26.4	0.51	0.048 5	1.5	0.162 2	2.5	0.025 3	0.7	161.2 ± 1.1	-695
TD133-11.2	1 108	587	24.3	0.53	0.050 2	2.0	0.166 9	3.1	0.025 5	0.7	162.2 ± 1.2	-118
TD133-12.1	258	91	5.56	0.35	0.048 2	3.8	0.151 1	5.3	0.025 0	1.3	159.0 ± 2.0	235

5 讨论

5.1 角闪石岩成因及源区

富角闪石基性-超基性岩(角闪石岩、角闪辉长岩、闪长岩)有相似岩石结构-构造,广泛出露于世界各地的造山带中并与花岗质岩石相伴产出(Kemp, 2004; Tiepolo and Tribuzio, 2008)。泽当岛弧角闪石岩产于花岗闪长岩下部,呈似层状产出,厚度较薄,显示为典型堆晶岩特征(图 2a)。角闪石岩与花岗闪长岩接触部位可见角闪石岩呈角砾状被花岗闪长岩脉体穿切,但二者接触面无烘烤边,说明二者可能近于同时形成于同一岩浆房(图 2b),且与岩浆混合作用下形成的暗色包体和岩浆上侵过程中围岩俘虏体的岩石学特征不同。锆石 U-Pb 年代学研究表明,角闪石岩形成于 159.1 ± 7.2 Ma, 花岗闪长岩形成于 157.5 ± 1.4 Ma(王莉等, 2012),支持角闪石岩结晶稍早于花岗闪长岩的推测。

矿物学研究表明,变质成因角闪石通常沿原生矿物解理或原生矿物颗粒间的缝隙生长,与原生矿物形成反应边结构或交代残余结构,自形程度较低,呈它形粒状结构,粒径较小(Jeff and Dante, 2010)。但是,泽当角闪石岩中角闪石自形程度较高,结晶较好,角闪石粒径较大(图 2c、2d),角闪石矿物学特征

与变质成因的角闪石有明显区别,应属岩浆成因。年代学、岩石学、矿物学三方面的研究表明,角闪石岩为岩浆分离结晶作用下形成的火成堆晶岩。

角闪石岩作为堆晶岩不能直接采用地球化学投图判别构造背景,但角闪石分离结晶作用不会导致 Sr-Nd 同位素的分馏,Sr-Nd 同位素特征仍然是角闪石岩源区的重要识别标志。此外,角闪石岩与高 Sr/Y 花岗岩同属泽当岛弧,两者产出关系密切,Sr-Nd 同位素比值接近,可能来自同一源区并存在岩浆演化关系,高 Sr/Y 花岗岩源区可以间接指示角闪石岩源区。

角闪石分离结晶作用对水具有类似于海绵的吸水作用(Davidson *et al.*, 2007)。实验岩石学研究显示,角闪石的稳定性随含水量的减少而降低(Jagoutz *et al.*, 2009),形成大规模的角闪石堆晶岩要求原始岩浆具有富水特征。岛弧环境中,不仅可以形成富水熔体(水饱熔体含水量可超过体积比 14%)(Grove *et al.*, 2003),而且熔体很难受到地壳物质混染,具有较为一致的同位素特征(McDermott *et al.*, 1993; Maurice *et al.*, 2012)。泽当岛弧微量元素原始地幔标准化蛛网(图 3b)中 Nb、Ta 相对 K、La 亏损且 Pb 具正异常,显示与俯冲有关的岛弧背景(Jagoutz *et al.*, 2009)。绝大多数研究者也认为泽当岛弧形成于洋壳俯冲背景,是洋内弧的残余部分

表3 角闪石岩 Sr-Nd 同位素组成

Table 3 Sr-Nd isotope composition of magmatic amphibolite

样品编号	TD133-2	TD133-3	TD133-4	TD133-5	TD133-6	TD133-7
w(Rb)/10 ⁻⁶	5.0	25.0	15.0	9.9	22.1	16.5
w(Sr)/10 ⁻⁶	1.150	449	478	355	541	442
Rb/Sr	0.004	0.056	0.031	0.028	0.041	0.037
⁸⁷ Rb/ ⁸⁶ Sr	0.012	0.161	0.091	0.081	0.118	0.108
⁸⁷ Sr/ ⁸⁶ Sr	0.704 3	0.704 7	0.704 2	0.704 7	0.704 7	0.704 6
($2s_m$)	0.000 011	0.000 011	0.000 012	0.000 014	0.000 011	0.000 011
w(Sm)/10 ⁻⁶	3.72	3.12	2.26	2.57	2.33	2.57
w(Nd)/10 ⁻⁶	17.4	11.9	8.4	9.4	8.3	8.6
Sm/Nd	0.214	0.262	0.269	0.273	0.281	0.299
¹⁴⁷ Sm/ ¹⁴⁴ Nd	0.129 3	0.158 5	0.162 7	0.165 8	0.168 9	0.180 5
¹⁴³ Nd/ ¹⁴⁴ Nd	0.512 882	0.512 903	0.512 886	0.512 896	0.512 898	0.512 902
($2s_m$)	0.000 006	0.000 007	0.000 007	0.000 005	0.000 008	0.000 008
ε Nd(t)	6.1	6.0	5.5	5.7	5.6	5.5
⁸⁷ Sr/ ⁸⁶ Sr(t)	0.704 3	0.704 4	0.704 0	0.704 5	0.704 4	0.704 4
¹⁴³ Nd/ ¹⁴⁴ Nd(t)	0.512 747	0.512 738	0.512 717	0.512 724	0.512 722	0.512 714

注: ${}^{87}\text{Sr}/{}^{86}\text{Sr}(t) = {}^{87}\text{Sr}/{}^{86}\text{Sr} - {}^{87}\text{Rb}/{}^{86}\text{Sr}(e^{\lambda t} - 1)$, 其中 $\lambda = 1.42 \times 10^{-11}/\text{a}$, $t = 159 \text{ Ma}$; ${}^{143}\text{Nd}/{}^{144}\text{Nd}(t) = {}^{143}\text{Nd}/{}^{144}\text{Nd} - {}^{143}\text{Sm}/{}^{144}\text{Nd}(e^{\lambda t} - 1)$; ${}^{143}\text{Nd}/{}^{144}\text{Nd}_{(\text{CHUR})} = {}^{143}\text{Nd}/{}^{144}\text{Nd} - {}^{143}\text{Sm}/{}^{144}\text{Nd}(e^{\lambda t} - 1)$; $\varepsilon\text{Nd}(t) = [({}^{143}\text{Nd}/{}^{144}\text{Nd}_{(\text{i})})/{}^{143}\text{Nd}/{}^{144}\text{Nd}_{(\text{CHUR})} - 1] \times 10^4$; 其中在计算 ${}^{143}\text{Nd}/{}^{144}\text{Nd}_{(\text{CHUR})}$ 时, ${}^{143}\text{Nd}/{}^{144}\text{Nd} = 0.512 638$, ${}^{143}\text{Sm}/{}^{144}\text{Nd} = 0.196 7$, $\lambda = 6.54 \times 10^{-11}/\text{a}$, $t = 159 \text{ Ma}$ 。

表4 泽当岛弧岩浆岩元素地球化学特征

Table 4 Element geochemical characteristics of Zetang island arc magmatic rocks

岩石类型	英云闪长岩	花岗闪长岩	奥长花岗岩	角闪石岩
w(SiO ₂)/%	57.98 ~ 63.69	64.42 ~ 68.43	64.83 ~ 68.33	44.49 ~ 47.92
w(K ₂ O)/w(Na ₂ O)	0.36 ~ 0.63	0.31 ~ 0.47	0.31 ~ 0.49	0.13 ~ 0.85
w(MgO)	0.69 ~ 1.08	0.76 ~ 1.16	0.67 ~ 1.17	6.55 ~ 14.87
Mg [#]	30 ~ 42	48 ~ 56	51 ~ 52	57 ~ 73
w(Cr)/10 ⁻⁶	94.3	31.5	12.5	576.0
w(Ni)/10 ⁻⁶	51.9	18.6	8.8	241.9
w(Sr)/w(Y)	77.0 ~ 106.7	114.4 ~ 220.8	84.5 ~ 205.6	23.8 ~ 74.7
⁸⁷ Sr/ ⁸⁶ Sr	0.704 8 ~ 0.705 0	0.704 5 ~ 0.704 9		0.704 2 ~ 0.704 7
¹⁴³ Nd/ ¹⁴⁴ Nd(t)	0.512 8	0.512 7 ~ 0.512 9		0.512 7
ε Nd(t)	+6.7 ~ +7.3	+5.1 ~ +6.1		+5.5 ~ +6.1

注: Mg[#] = 100 × n(Mg²⁺) / n(Mg²⁺ + Fe²⁺); 英云闪长岩数据引自韦栋梁等(2007); 花岗闪长岩数据引自王莉等(2012); 奥长花岗岩数据引自赵珍等(2014)。

(Aitchison *et al.*, 2000, 2007; McDermid *et al.*, 2002; 韦栋梁等, 2007; 王莉等, 2012; 赵珍等, 2014)。

前人对泽当岛弧高 Sr/Y 花岗岩的源区存在两种观点: 俯冲板片部分熔融(韦栋梁等, 2007; 赵珍等, 2014)和地幔楔部分熔融体板底垫托作用下, 新生下地壳熔融(王莉等, 2012)。前已述及, 堆晶成因的角闪石岩的元素地球化学特征不能用来判断其来源, 需借助同来源的花岗质岩石进行判定。泽当岛弧稀土元素球粒陨石标准化图(图 3a)显示, 英云闪长岩具有 Eu 正异常, 花岗闪长岩和奥长花岗岩具

有 Eu 负异常, 说明花岗闪长岩和奥长花岗岩演化程度更高, 已经发生斜长石分离结晶作用, 英云闪长岩可能源于更原始的富水岩浆, 对源区的指示更有代表性。

英云闪长岩的 Th/La > 0.2, Th/Yb > 2, 具有板片俯冲沉积物特征(Seghedi *et al.*, 2001; Elburg *et al.*, 2002; Plank, 2005)。俯冲板片熔体上侵过程中会与地幔楔橄榄岩发生再平衡作用, 形成高镁安山岩(Mg[#] > 60)和对应的侵入岩(Kay, 1978; Wood and Turner, 2009), 但英云闪长岩 Mg[#] 值较低, Sr、Ba、Ni 含量较高。研究显示, 俯冲带高压环境下, 斜

长石不稳定,有利于Sr、Ba的释放(Chapman *et al.*, 2015),流体能将大量Sr、Ba从榴辉岩化洋壳和沉积物中运移至岩石圈地幔(Hermann and Rubatto, 2009),导致俯冲带岩浆岩中Sr、Ba含量增加(Vigouroux *et al.*, 2008),英云闪长岩中高Sr、Ba特征可能是由于源区中富Sr、Ba流体的加入所致。同时,幔源熔体分离结晶作用是形成高Ni花岗岩的主要机制,而单纯的地壳物质部分熔融很难形成此种高Ni地球化学特征(Jagoutz *et al.*, 2009)。英云闪长岩显示高Ni(22.4×10^{-6} ~ 165.8×10^{-6})特征,符合交代地幔楔熔融的特征。

本次研究认为,地幔楔在受到大洋板片富水流体交代作用下可能发生水致熔融(Grove *et al.*, 2002; Jagoutz *et al.*, 2011),并演化形成具有高Ni(22.4×10^{-6} ~ 165.8×10^{-6})、高Sr(810.5×10^{-6} ~ 943.2×10^{-6})和高Ba(809.9×10^{-6} ~ 2049.3×10^{-6})地球化学的熔体。此种富水的幔源碱性-钙碱性玄武质熔体发生以角闪石为主的分离结晶作用,形成富钠、高Sr/Y长英质岩浆(Jagoutz *et al.*, 2011; Smithies *et al.*, 2019)。因此,角闪石岩源区可能属交代地幔楔,其可能为地幔楔熔融岩浆在演化过程中发生分离结晶的产物。

5.2 泽当岛弧高Sr/Y花岗岩成因机制

高Sr/Y花岗岩形成机制主要有:①俯冲洋壳部分熔融(Defant and Drummond, 1990);②增厚下地壳或拆沉下地壳部分熔融(Rapp *et al.*, 2002; Wang *et al.*, 2004; Xu *et al.*, 2004; Zhou *et al.*, 2006; Ding *et al.*, 2007; Xiao *et al.*, 2007);③长英质岩浆与玄武质岩浆的混合作用(Guo *et al.*, 2007; Streck *et al.*, 2007; Qin *et al.*, 2007);④岩浆的分离结晶作用(Castillo *et al.*, 1999; Castillo, 2006; Moyen, 2009)。在泽当岛弧,英云闪长岩、花岗闪长岩和奥长花岗岩三者形成时代接近,地球化学特征具有相似性,三者皆为富Na($\text{Na}_2\text{O} \gg \text{K}_2\text{O}$)、高Sr($\text{Sr} > 300 \times 10^{-6}$)、低Y及高Sr/Y值(平均122.9)、富集LILE、亏损HFSE特征的花岗岩。俯冲洋壳部分熔融和拆沉下地壳过程形成的高Sr/Y花岗岩具有高MgO和高Mg[#]的特征,这是由于俯冲板片直接熔融形成的熔体和拆沉下地壳部分熔融形成的熔体与地幔橄榄岩发生交代/混染作用,使MgO和Mg[#]升高(许继峰等, 2014; 郑永飞等, 2016)。增厚下地壳熔融条件下形成的高Sr/Y花岗岩往往具有高K₂O、高K/Na值(0.7~2.0)、负的εNd(t)值、

较高的⁸⁷Sr/⁸⁶Sr(t)和极低的Mg[#]值(约40)(Moyen, 2009; 郑永飞等, 2015)。①和②过程所处的高温高压环境,可以形成石榴角闪岩或榴辉岩(Richards and Kerrich, 2007),部分熔融作用中石榴子石作为残留相存在(Wyllie *et al.*, 1989; Poli and Schmidt, 2002; Grove *et al.*, 2006)。石榴子石强烈富集HREE(Nicholls and Harris, 1980; Sisson and Bacon, 1992; Van Westrenen *et al.*, 1999; Rubatto and Hermann, 2007),会导致高Sr/Y花岗岩LREE和HREE严重分异。泽当岛弧高Sr/Y花岗岩具有低K₂O、低K/Na、正εNd(t)、低⁸⁷Sr/⁸⁶Sr(t)、低MgO、低Mg[#]的特征,据此可以排除成因①和②。弧晚期阶段,可能发生③玄武质岩浆底侵造成的下地壳部分熔融作用或者玄武岩质岩浆与长英质岩浆混合作用(Taylor and McLennan, 1985; Rudnick and Gao, 2003; Tatsumi *et al.*, 2008)。玄武岩质岩浆与长英质岩浆混合会产生大量包体(董国臣等, 2006; 王德滋等, 2008)。岩浆混合作用还会导致早期结晶矿物出现残核结构、文象结构、蠕虫结构和交代结构等(李昌年, 2002; 齐有强等, 2008)。

泽当角闪石岩及泽当岛弧高Sr/Y花岗岩(McDermid *et al.*, 2002; 韦栋梁等, 2007; 王莉等, 2012; 赵珍等, 2014)研究中并未发现上述与岩浆混合作用有关的岩石学、矿物学证据。岩浆混合作用还会导致岩浆Sr-Nd同位素特征因地壳物质的加入而出现较大的变化区间,泽当岛弧侵入岩Sr-Nd同位素数值较为均一,变化范围很小。泽当岛弧侵入岩εNd(t)-SiO₂关系图显示(图5),样品εNd(t)值和SiO₂含量没有明显线性相关性,说明泽当岛弧侵入岩形成过程中没有发生玄武质岩浆与长英质岩浆混合作用。

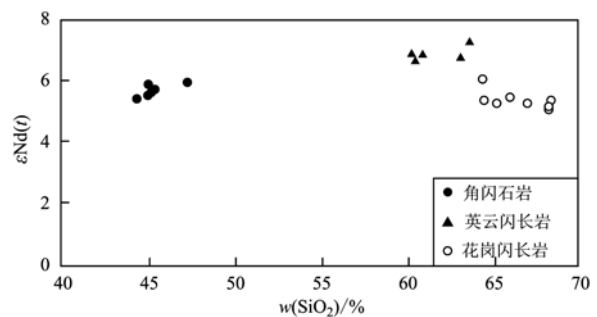


图5 泽当岛弧侵入岩εNd(t)-SiO₂关系图

Fig. 5 εNd(t)-SiO₂ diagram of Zetang island arc intrusion

实验岩石学研究表明,玄武-安山质熔体体系到英安岩-流纹岩熔体体系,微量元素Sr在普通角闪石与熔体之间的分配系数始终小于1,且逐渐降低(0.46~0.20),Y元素在角闪石和熔体之间的分配系数逐渐增高(1~6)(Rollison, 1993),这说明随着岩浆演化程度增高,如果熔体中发生大量角闪石分

离结晶作用,角闪石会富集微量元素Y和MREE,导致残余熔体中Y大量亏损,Sr少量富集,Sr/Y值升高(Gromet and Silver, 1987; Klein *et al.*, 1997; Bachmann *et al.*, 2005; Prowatke and Klemme, 2006)。因此,角闪石分离结晶(图6)可能是泽当岛弧花岗岩出现高Sr/Y值特征的主要原因。

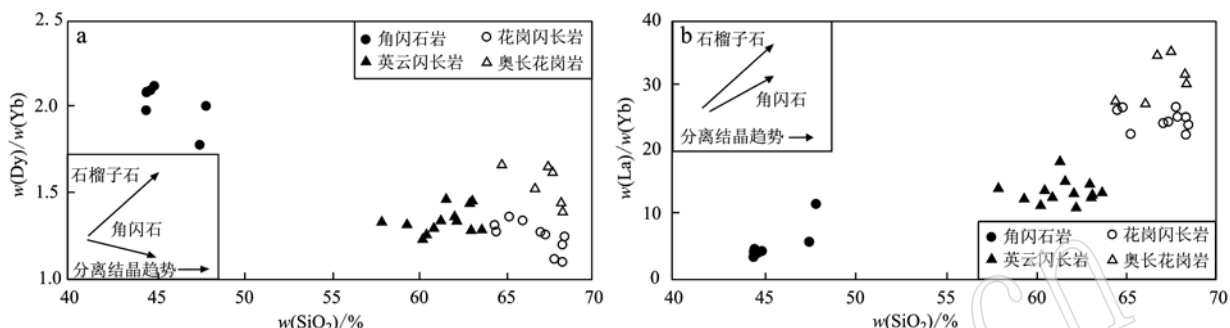


图6 泽当岛弧侵入岩 Dy/Yb - SiO₂ 和 La/Yb - SiO₂ 关系图解(底图据 Davidson *et al.*, 2007)

Fig. 6 Dy/Yb - SiO₂ and La/Yb - SiO₂ diagrams of Zetang island arc intrusion (after Davidson *et al.*, 2007)

前人研究数据显示,奥长花岗岩和花岗闪长岩Sr/Y值接近,英云闪长岩Sr/Y值略低于二者,但英云闪长岩中Y元素含量是二者的1.2~2.0倍。英云闪长岩中MREE、Cr、Ni含量高于奥长花岗岩和花岗闪长岩,说明三者受角闪石分离结晶作用的影响程度不同。微量元素地球化学特征和三者形成的先后顺序(年代学研究)显示,泽当岛弧侵入岩原始岩浆形成后发生显著的角闪石分离结晶作用,先形成高Sr/Y英云闪长岩,在角闪石分离结晶作用未结束前,英云闪长岩可能先从母岩浆中分离出去,残余岩浆继续发生角闪石分离结晶作用,形成高Sr/Y花岗闪长岩和高Sr/Y奥长花岗岩。上述过程导致晚期形成的花岗闪长岩和奥长花岗岩中MREE含量小于早期的英云闪长岩,并造成晚期的花岗闪长岩和奥长花岗岩中Cr、Ni、Y含量降低以及Sr/Y比值进一步升高。

6 结论

(1) 泽当岛弧角闪石岩岩石学和矿物学研究表明,角闪石岩为分离结晶作用下形成的火成堆晶岩,可能是地幔楔熔融岩浆演化过程中分离结晶作用的产物。

(2) 泽当岛弧角闪石岩与高Sr/Y花岗岩在产出关系和同位素地球化学特征上具有明显的成因联

系,综合研究认为泽当岛弧侵入岩源区可能为地幔楔。

(3) 泽当岛弧高Sr/Y花岗岩微量元素地球化学和投图结果显示,其经历了显著的角闪石分离结晶作用,角闪石分离结晶作用可能是导致花岗岩中Sr/Y值升高和MREE含量降低的主要原因。

References

- Aitchison J C, McDermid I R C, Ali J R, *et al.* 2007. Shoshonites in southern Tibet record Late Jurassic rifting of a Tethyan intraoceanic island arc[J]. Journal of Geology, 115(2): 197~213.
- Aitchison J C, Zhu B D, Davis A M, *et al.* 2000. Remnants of a Cretaceous intra-oceanic subduction system within the Yarlung-Zangbo suture (southern Tibet)[J]. Earth and Planetary Science Letters, 183(1): 231~244.
- Arbaret L, Burg J P, Zeilinger G, *et al.* 2000. Pre-collisional anastomosing shear zones in the Kohistan arc, NW Pakistan[J]. Geological Society, 170(1): 295~311.
- Bachmann O, Dungan M A and Bussy F. 2005. Insights into shallow magmatic processes in large silicic magma bodies: The trace element record in the Fish Canyon magma body, Colorado[J]. Contributions to Mineralogy and Petrology, 149(3): 338~349.
- Bard J P. 1983. Metamorphism of an obducted island arc: Example of the Kohistan sequence (Pakistan) in the Himalayan collided range[J].

- Earth and Planetary Science Letters, 65 (1): 133 ~ 144.
- Burg J P. 2011. The Asia-Kohistan-India collision: Review and discussion [A]. Brown D and Ryan P D. Arc-continent Collision, Frontiers in Earth Sciences[C]. Springer-Verlag Berlin Heidelberg, 279 ~ 309.
- Burg J P, Bodinier J L, Chaudhry S, et al. 1998. Infra-arc mantle-crust transition and intra-arc mantle diapirs in the Kohistan Complex (Pakistani Himalaya): Petro-structural evidence[J]. Terra Nova, 10 (2): 74 ~ 80.
- Castillo P. 2006. An overview of adakite petrogenesis[J]. Chinese Science Bulletin, 51 (3): 257 ~ 268.
- Castillo P R, Janney P E and Solidum R U. 1999. Petrology and geochemistry of Camiguin Island, southern Philippines: Insights to the source of adakites and other lavas in a complex arc setting[J]. Contributions to Mineralogy & Petrology, 134 (1): 33 ~ 51.
- Chapman J B, Ducea M N, Decelles P G, et al. 2015. Tracking changes in crustal thickness during orogenic evolution with Sr/Y: An example from the North American Cordillera[J]. Geology, 43(3): 919 ~ 922.
- Chen F K, Hegner E and Todt W. 2000. Zircon ages, Nd isotopic and chemical compositions of orthogneisses from the Black Forest, Germany: Evidence for a Cambrian magmatic arc[J]. International Journal of Earth Sciences, 88: 791 ~ 802.
- Chen F K, Li X H, Wang X L, et al. 2007. Zircon age and Nd-Hf isotopic composition of the Yunnan Tethyan belt, southwestern China [J]. International Journal of Earth Sciences, 96: 1 179 ~ 1 194.
- Chen F K, Siebel W, Satir M, et al. 2002. Geochronology of the Karadare basement (NW Turkey) and implications for the geological evolution of the Istanbul zone[J]. International Journal of Earth Sciences, 91: 469 ~ 481.
- Davidson J, Turner S, Handley H, et al. 2007. Amphibole “sponge” in arc crust? [J]. Geology, 35(9): 787 ~ 790.
- DeBari S M and Coleman R G. 1989. Examination of the deep levels of an island arc: Evidence from the Tonsina ultramafic-mafic assemblage [J]. Journal of Geophysical Research, 94 (B4): 4 373 ~ 4 391.
- DeBari S M and Greene A R. 2011. Vertical stratification of composition, density, and inferred magmatic processes in exposed arc crustal sections [A]. Brown D and Ryan P D. Arc-Continent Collision, Frontiers in Earth Sciences[C]. Springer-Verlag Berlin Heidelberg, 121 ~ 144.
- Defant M J and Drummond M S. 1990. Derivation of some modern arc magmas by melting of young subducted lithosphere[J]. Nature, 347 (6 294): 662 ~ 665.
- Dhuime B, Bosch D, Bodinier J L, et al. 2007. Multistage evolution of the Jijal ultramafic-mafic complex (Kohistan, N Pakistan): Implications for building the roots of island arcs[J]. Earth and Planetary Science Letters, 261 (1 ~ 2): 179 ~ 200.
- Ding Lin, Kapp P, Yue Y H, et al. 2007. Postcollisional calc-alkaline lavas and xenoliths from the Southern Qiangtang terrane, central Tibet [J]. Earth and Planetary Science Letters, 254 (1 ~ 2): 28 ~ 38.
- Dong Guochen, Mo Xuanxue, Zhao Zhidan, et al. 2006. Magma mixing in middle part of Gangdise magma belt: Evidences from granitoid complex[J]. Acta Petrologica Sinica, 22 (4): 835 ~ 844 (in Chinese with English abstract).
- Elburg M A, Bergen M V, Hoogewerff J, et al. 2002. Geochemical trends across an arc-continent collision zone: magma sources and slab-wedge transfer processes below the Pantar Strait volcanoes, Indonesia [J]. Geochimica et Cosmochimica Acta, 66(15): 2 771 ~ 2 789.
- Garrido C J, Bodinier J L, Burg J P, et al. 2006. Petrogenesis of mafic garnet granulite in the lower crust of the Kohistan paleo-arc complex (northern Pakistan): Implications for intra-crustal differentiation of island arcs and generation of continental crust[J]. Journal of Petrology, 47 (10): 1 873 ~ 1 914.
- Greene A R, DeBari S M, Kelemen P B, et al. 2006. A detailed geochemical study of island arc crust: The Talkeetna arc section, south-central Alaska[J]. Journal of Petrology, 47 (6): 1 051 ~ 1 093.
- Cromet L P and Silver L T. 1987. REE Variations across the Peninsular Ranges batholith: Implications for batholithic petrogenesis and crustal growth in magmatic arcs[J]. Journal of Petrology, 28 (1): 75 ~ 125.
- Grove T L, Chatterjee N, Parman S W, et al. 2006. The influence of H_2O on mantle wedge melting[J]. Earth and Planetary Science Letters, 249 (1 ~ 2): 74 ~ 89.
- Grove T L, Elkins-Tanton L T, Parman S W, et al. 2003. Fractional crystallization and mantle-melting controls on calc-alkaline differentiation trends[J]. Contributions to Mineralogy and Petrology, 145(5): 515 ~ 533.
- Grove T, Parman S, Bowring S, et al. 2002. The role of an H_2O -rich fluid component in the generation of primitive basaltic andesites and andesites from the Mt. Shasta region, N California[J]. Contributions to Mineralogy and Petrology, 142(4): 375 ~ 396.
- Guo Z F, Wilson M and Liu J Q. 2007. Post-collisional adakites in south Tibet: Products of partial melting of subduction-modified lower crust [J]. Lithos, 96 (1 ~ 2): 205 ~ 224.
- Harrison T M, Yin A, Grove M, et al. 2000. The Zedong Window: A record of superposed Tertiary convergence in southeastern Tibet[J]. Journal of Geophysical Research: Solid Earth, 105(B8).
- Hermann J and Rubatto D. 2009. Accessory phase control on the trace element signature of sediment melts in subduction zones[J]. Chemical Geology, 265(3 ~ 4): 512 ~ 526.
- Isacks B, Oliver J and Sykes L R. 1968. Seismology and the new global

- tectonics[J]. *Journal of Geophysical Research*, 73: 5 855 ~ 5 899.
- Jagoutz O E, Burg J P, Hussain S, et al. 2009. Construction of the granitoid crust of an island arc part I: Geochronological and geochemical constraints from the plutonic Kohistan (NW Pakistan)[J]. *Contributions to Mineralogy and Petrology*, 158(6): 739 ~ 755.
- Jagoutz O, Othmar Müntener, Schmidt M W, et al. 2011. The roles of flux- and decompression melting and their respective fractionation lines for continental crust formation: Evidence from the Kohistan arc[J]. *Earth and Planetary Science Letters*, 303(1 ~ 2): 25 ~ 36.
- Jeff L and Dante C. 2010. The role of amphibole in the evolution of arc magmas and crust: The case from the Jurassic Bonanza arc section, Vancouver Island, Canada[J]. *Contributions to Mineralogy and Petrology*, 159(4): 475 ~ 492.
- Ji Ang. 2012. Development of X-ray fluorescence spectrometry in the 30 years[J]. *Rock and Mineral Analysis*, 31(3): 383 ~ 398 (in Chinese with English abstract).
- Kay R W. 1978. Aleutian magnesian andesites: Melts from subducted Pacific ocean crust[J]. *Journal of Volcanology and Geothermal Research*, 4: 117 ~ 132.
- Kelemen P B, Hanghøj K, Greene A R, et al. 2007. One view of the geochemistry of subduction-related magmatic arcs, with an emphasis on primitive andesite and lower crust[J]. *Treatise on Geochemistry*, 3: 1 ~ 70.
- Kemp A I S. 2004. Petrology of high-Mg, low-Ti igneous rocks of the Glenelg River Complex (SE Australia) and the nature of their interaction with crustal melts[J]. *Lithos*, 78: 119 ~ 156.
- Klein M, Stosch H G and Seck H A. 1997. Partitioning of high field-strength and rare-earth elements between amphibole and quartz-dioritic to tonalitic melts: An experimental study[J]. *Chemical Geology*, 138 (3 ~ 4): 257 ~ 271.
- Lang X H, Tang J X, Li Z J, et al. 2014. U-Pb and Re-Os geochronological evidence for the Jurassic porphyry metallogenetic event of the Xiong-cun district in the Gangdese porphyry copper belt, southern Tibet, PRC[J]. *Journal of Asian Earth Sciences*, 79 (B): 608 ~ 622.
- Li Changnian. 2002. Comment on the magma mixing and their research [J]. *Geological Science and Technology Information*, 21 (4): 49 ~ 54 (in Chinese with English abstract).
- Li Qiang, Xia Bin, Huang Qiangtai, et al. 2014. The origin and evolution of Zedang ophiolite in the Eastern Yarlung-Zangbo Suture Zone, Southern Tibet[J]. *Acta Geologica Sinica*, 88(2): 145 ~ 166 (in Chinese with English abstract).
- Liu Weiliang, Xian Bin, Liu Hongfei, et al. 2013. U-Pb dating of basalt from Zéting ophiolite in Tibet and its geological implications[J]. *Geological Bulletin of China*, 32(9): 1 356 ~ 1 361 (in Chinese with English abstract).
- Ludwig K R. 2003. User's Manual for ISOPLOT 3.00: A Geochronological Toolkit for Microsoft Excel[M]. California: Berkeley Geochronology Center, 41 ~ 70.
- Maurice A E, Basta F F and Khiamy A A. 2012. Neoproterozoic nascent island arc volcanism from the Nubian Shield of Egypt: Magma genesis and generation of continental crust in intra-oceanic arcs[J]. *Lithos*, 132: 1 ~ 20.
- McDermid I R C, Aitchison J C, Davis A M, et al. 2002. The Zedong terrane: A Late Jurassic intra-oceanic magmatic arc within the Yarlung-Tsangpo suture zone, southeastern Tibet [J]. *Chemical Geology*, 187(3): 267 ~ 277.
- McDermott F, Defant M J, Hawkesworth C J, et al. 1993. Isotope and trace element evidence for three component mixing in the genesis of the North Luzon arc lavas (Philippines)[J]. *Contributions to Mineralogy and Petrology*, 113: 9 ~ 23.
- McDonough W F and Sun S S. 1995. The composition of the Earth[J]. *Chemical Geology*, 120 (3 ~ 4): 223 ~ 253.
- Moyen J F. 2009. High Sr/Y and La/Yb ratios: The meaning of the "adakitic signature" [J]. *Lithos*, 112(3 ~ 4): 556 ~ 574.
- Nicholls I A and Harris K L. 1980. Experimental rare earth element partitioning coefficients for garnet, clinopyroxene and amphibole coexisting with andesitic and basaltic liquids[J]. *Geochimica et Cosmochimica Acta*, 44 (2): 287 ~ 308.
- Oliver J and Isacks B. 1967. Deep earthquake zones, anomalous structures in the upper mantle, and lithosphere[J]. *Journal of Geophysical Research*, 72 (16): 4 259 ~ 4 275.
- Plank T. 2005. Constraints from thorium/lanthanum sediment recycling at subduction zones and the evolution of the continents[J]. *Journal of Petrology*, 46(5): 921 ~ 944.
- Poli S and Schmidt M W. 2002. Petrology of subducted slabs[J]. *Annual Reviews of Earth and Planetary Sciences*, 30 (30): 207 ~ 235.
- Prowatke S and Klemme S. 2006. Rare earth element partitioning between titanite and silicate melts: Henry's law revisited[J]. *Geochimica et Cosmochimica Acta*, 70 (19): 4 997 ~ 5 012.
- Qi Youqiang, Hu Ruizhong, Liu Shen, et al. 2008. Review on magma mixing and mingling[J]. *Bulletin of Mineralogy, Petrology and Geochemistry*, 27 (4): 409 ~ 416 (in Chinese with English abstract).
- Qin J F, Lai S C and Wang J. 2007. High-Mg[#] adakitic tonalite from the Xichahe area, south Qinling Orogenic Belt (Central China): Petrogenesis and geological implications[J]. *International Geology Review*, 49 (12): 1 145 ~ 1 158.
- Quidelleur X, Grove M, Lovera O M, et al. 1997. Thermal evolution and slip history of the Renbu-Zedong Thrust, southeastern Tibet[J]. *Journal of Geophysical Research*, 102 (B2): 2 659 ~ 2 679.

- Rapp R P, Xiao Long, Shimizu N. 2002. Experimental constraints on the origin of potassium-rich adakites in eastern China[J]. *Acta Petrologica Sinica*, 18 (3): 293 ~ 302.
- Richards J P and Kerrich R. 2007. Adakite-like rocks: Their diverse origins and questionable role in metallogenesis[J]. *Economic Geology*, 102(4): 537 ~ 576.
- Rollison H R. 1993. Using Geochemical Data: Evaluation, Presentation, Interpretation[M]. UK: Pearson Education Limited, 1 ~ 275.
- Rubatto D and Hermann J. 2007. Experimental zircon/melt and zircon/garnet trace element partitioning and implications for the geochronology of crustal rocks[J]. *Chemical Geology*, 241 (1 ~ 2): 38 ~ 61.
- Rudnick R L and Gao S. 2003. Composition of the continental crust[A]. Rudnick R L. *The Crust, Treatise on Geochemistry*[C]. 3: 1 ~ 70.
- Seghedi I, Downes H, Peckay Z, et al. 2001. Magmagenesis in a subduction-related post-collisional volcanic arc segment: The Ukrainian Carpathians[J]. *Lithos*, 57(4): 237 ~ 262.
- Sisson T W and Bacon C R. 1992. Garnet/high-silica rhyolite trace element partition coefficients measured by ion microprobe[J]. *Geochimica et Cosmochimica Acta*, 56 (5): 2 133 ~ 2 136.
- Smith D J. 2014. Clinopyroxene precursors to amphibole sponge in arc crust[J]. *Nature Communications*, 5: 1 ~ 6.
- Smith I E M and Price R C. 2006. The Tonga-Kermadec arc and Havre-Lau back-arc system: Their role in the development of tectonic and magmatic models for the western Pacific[J]. *Journal of Volcanology and Geothermal Research*, 156 (3): 315 ~ 331.
- Smithies R H, Lu Y J, Johnson T E, et al. 2019. No evidence for high-pressure melting of Earth's crust in the Archean[J]. *Nature Communications*, 10(1): 5 559.
- Song Biao. 2015. SHRIMP zircon U-Pb age measurement: Sample preparation, measurement, data processing and explanation[J]. *Geological Bulletin of China*, 34 (10): 1 777 ~ 1 788(in Chinese with English abstract).
- Stern R J, Fouch M J and Klemperer S L. 2003. An overview of the Izu-Bonin-Mariana subduction factory[J]. *Inside the Subduction Factory*, 138: 175 ~ 222.
- Streck M J, Leeman W P and Chesley J. 2007. High-magnesian andesite from Mount Shasta: A product of magma mixing and contamination, not a primitive mantle melt[J]. *Geology*, 35 (4): 351 ~ 354.
- Taylor S R and McLennan S M. 1985. The Continental Crust: Its Composition and Evolution: An Examination of the Geochemical Record Preserved in Sedimentary Rocks[M]. Blackwell Scientific Publications.
- Tatsumi Y, Shukuno H, Tani K, et al. 2008. Structure and growth of the Izu-Bonin-Mariana arc crust: 2. Role of crust-mantle transformation and the transparent Moho in arc crust evolution[J]. *Journal of Geophysical Research*, 113: B(2).
- Takahashi N, Kodaira S, Klemperer S L, et al. 2007. Crustal structure and evolution of the Mariana intra-oceanic island arc[J]. *Geology*, 35 (3): 203 ~ 206.
- Takahashi N, Kodaira S, Tatsumi Y, et al. 2008. Structure and growth of the Izu-Bonin-Mariana arc crust: 1. Seismic constraint on crust and mantle structure of the Mariana arc-back-arc system[J]. *Journal of Geophysical Research*, 113 (B1): 699 ~ 701.
- Tang J X, Lang X H, Xie F W, et al. 2015. Geological characteristics and genesis of the Jurassic No. I porphyry Cu-Au deposit in the Xiongeun district, Gangdese porphyry copper belt, Tibet[J]. *Ore Geology Reviews*, 70: 438 ~ 456.
- Tiepolo M and Tribuzio R. 2008. Petrology and U-Pb zircon geochronology of amphibole-rich cumulates with samukitic affinity from Husky Ridge (Northern Victoria Land, Antarctica): Insights into the role of amphibole in the petrogenesis of subduction-related magmas[J]. *Journal of Petrology*, 49: 937 ~ 970.
- Van Westrenen W, Blundy J and Wood B. 1999. Crystal-chemical controls on trace element partitioning between garnet and anhydrous silicate melt[J]. *American Mineralogist*, 84(5 ~ 6): 838 ~ 847.
- Vigouroux N, Wallace P J and Kent A J R. 2008. Volatiles in high-K magmas from the western Trans-Mexican Volcanic Belt: Evidence for fluid fluxing and extreme enrichment of the mantle wedge by subduction processes[J]. *Journal of Petrology*, 49(9): 12 ~ 15.
- Wang Dezi and Xie Lei. 2008. Magma mingling: Evidence from enclaves [J]. *Geological Journal of China Universities*, 14 (1): 16 ~ 21(in Chinese with English abstract).
- Wang Li, Zeng Lingsen, Gao Li'e, et al. 2012. Remnant Jurassic intra-oceanic arc system in Southern Tibet: Geochemistry and tectonic implications[J]. *Acta Petrologica Sinica*, 28 (6): 1 741 ~ 1 754 (in Chinese with English abstract).
- Wang Q, Xu J F, Zhao Z H, et al. 2004. Cretaceous high-potassium intrusive rocks in the Yuesha-Hongzhen area of east China: Adakites in an extensional tectonic regime within a continent[J]. *Geochemical Journal*, 38(5): 417 ~ 434.
- Wei Dongliang, Xia Bin, Zhou Guoqing, et al. 2004. Lithochemical characteristics and origin of the Zedang ophiolite lava in Xizang (Tibet), China[J]. *Geotectonica et Metallogenesis*, 28 (3): 270 ~ 278 (in Chinese with English abstract).
- Wei Dongliang, Xia Bin, Zhou Guoqing, et al. 2006. Sm-Nd isochron age of Zedang ophiolite in Tibet and its significance[J]. *Acta Geoscientifica Sinica*, 27 (1): 31 ~ 34 (in Chinese with English abstract).
- Wei Dongliang, Xia Bin, Zhou Guoqing, et al. 2007. Geochemical and Sr-Nd isotopic characteristics of Zedang tonalite, Tibet: New evidence of Tethys subduction[J]. *Science China (Earth Sciences)*, 37 (4):

- 442~450(in Chinese with English abstract).
- Wood B J and Turner S. 2009. Origin of primitive high-Mg andesite: constraints from natural examples and experiments[J]. *Earth and Planetary Science Letters*, 283: 59~66.
- Wyllie P J, Carroll M R, Johnston A D, et al. 1989. Interactions among magmas and rocks in subduction zone regions: Experimental studies from slab to mantle to crust[J]. *European Journal of Mineralogy*, 1(2): 165~179.
- Xiao L, Zhang F H, Clemens J D, et al. 2007. Late Triassic granitoids of the eastern margin of the Tibetan Plateau: Geochronology, petrogenesis and implications for tectonic evolution[J]. *Lithos*, 96(3): 436~452.
- Xu Jifeng, Wu Jianbin, Wang Qiang, et al. 2014. Research advances of adakites and adakitic rocks in China[J]. *Bulletin of Mineralogy, Petrology and Geochemistry*, 33(1): 6~13(in Chinese with English abstract).
- Xu Y G, Huang X L, Ma J L, et al. 2004. Crust-mantle interaction during the tectono-thermal reactivation of the North China Craton: Constraints from SHRIMP zircon U-Pb chronology and geochemistry of Mesozoic plutons from Western Shandong[J]. *Contributions to Mineralogy and Petrology*, 147(6): 750~767.
- Yin An, Harrison T M, Murphy M A, et al. 1999. Tertiary deformation history of southeastern and southwestern Tibet during the Indo-Asian collision[J]. *Geological Society of America Bulletin*, 111(11): 1644.
- Yin An, Harrison T M, Ryerson F J, et al. 1994. Tertiary structural evolution of the Gangdese thrust system in southeastern Tibet[J]. *Journal of Geophysical Research*, 99(B9): 18 175~18 201.
- Zhang L L, Liu C Z, Wu F Y, et al. 2014. Zedang terrane revisited: An intra-oceanic arc within Neo-Tethys or a part of the Asian active continental margin? [J]. *Journal of Asian Earth Sciences*, 80(2): 34~55.
- Zhao Zhen, Wu Zhenhan, Hu Daogong, et al. 2014. Multistage magmatism of the Zetang polymetallic orefield on the southern margin of the Gangdise belt in the Tibetan plateau and its chronological significance[J]. *Acta Geoscientica Sinica*, 35(6): 703~712(in Chinese with English abstract).
- Zheng Yongfei, Chen Renxu, Xu Zheng, et al. 2016. The transport of water in subduction zones[J]. *Science China Earth Sciences*, 59: 651~681.
- Zheng Yongfei, Chen Yixiang, Dai Liqun, et al. 2015. Developing plate tectonics theory from oceanic subduction zones to collisional orogens[J]. *Science China: Earth Sciences*, 58: 1 045~1 069.
- Zhou Meifu, Yan Daping, Wang Changliang, et al. 2006. Subduction-related origin of the 750 Ma Xuelongbao adakitic complex (Sichuan Province, China): Implications for the tectonic setting of the giant Neoproterozoic magmatic event in South China[J]. *Earth and Planetary Science Letters*, 248(1~2): 286~300.
- Zhuo Shangjun and Ji Ang. 2003. Progress in X-ray fluorescence analysis [J]. *Chinese Journal of Analysis Laboratory*, 22(3): 102~108(in Chinese with English abstract).
- ### 附中文参考文献
- 董国臣, 莫宣学, 赵志丹, 等. 2006. 冈底斯岩浆带中段岩浆混合作用: 来自花岗杂岩的证据[J]. *岩石学报*, 22(4): 835~844.
- 吉 昂. 2012. X射线荧光光谱三十年[J]. *岩矿测试*, 31(3): 383~398.
- 李昌年. 2002. 岩浆混合作用及其研究评述[J]. *地质科技情报*, 21(4): 49~54.
- 李 强, 夏 斌, 黄强太, 等. 2014. 雅鲁藏布江蛇绿岩带东段泽当蛇绿岩起源及演化[J]. *地质学报*, 88(2): 145~166.
- 刘维亮, 夏 斌, 刘鸿飞, 等. 2013. 西藏泽当蛇绿岩玄武岩 SHRIMP 锆石 U-Pb 年龄及其地质意义[J]. *地质通报*, 32(9): 1 356~1 361.
- 齐有强, 胡瑞忠, 刘 瑞, 等. 2008. 岩浆混合作用研究综述[J]. *矿物岩石地球化学通报*, 27(4): 409~416.
- 宋 彪. 2015. 用 SHRIMP 测定锆石 U-Pb 年龄的工作方法[J]. *地质通报*, 34(10): 1 777~1 788.
- 王德滋, 谢 磊. 2008. 岩浆混合作用: 来自岩石包体的证据[J]. *高校地质学报*, 14(1): 16~21.
- 王 莉, 曾令森, 高利娥, 等. 2012. 藏南侏罗纪残留洋弧的地球化学特征及其大地构造意义[J]. *岩石学报*, 28(6): 1 741~1 754.
- 韦栋梁, 夏 斌, 周国庆, 等. 2004. 西藏泽当蛇绿岩壳层火山熔岩的岩石地球化学及成因[J]. *大地构造与成矿学*, 28(3): 270~278.
- 韦栋梁, 夏 斌, 周国庆, 等. 2006. 西藏泽当蛇绿岩的 Sm-Nd 等时线年龄及其意义[J]. *地球学报*, 27(1): 31~34.
- 韦栋梁, 夏 斌, 周国庆, 等. 2007. 西藏泽当英云闪长岩的地球化学和 Sr-Nd 同位素特征: 特提斯洋内俯冲的新证据[J]. *中国科学(D辑)*, 37(4): 442~450.
- 许继峰, 邬建斌, 王 强. 2014. 埃达克岩与埃达克质岩在中国的研究进展[J]. *矿物岩石地球化学通报*, 33(1): 6~13.
- 赵 珍, 吴珍汉, 胡道功, 等. 2014. 青藏高原冈底斯带南缘泽当多金属矿田多期岩浆活动及年代意义[J]. *地球科学*, 35(6): 703~712.
- 郑永飞, 陈仁旭, 徐 峥, 等. 2016. 俯冲带中的水迁移[J]. *中国科学: 地球科学*, 46(3): 253~286.
- 郑永飞, 陈伊翔, 戴立群, 等. 2015. 发展板块构造理论: 从洋壳俯冲带到碰撞造山带[J]. *中国科学: 地球科学*, 45(6): 711~735.
- 卓尚军, 吉 昂. 2003. X射线荧光光谱分析[J]. *分析实验室*, 22(3): 102~108.